Divergent selection for residual feed intake affects the transcriptomic and proteomic profiles of pig skeletal muscle

Annie Vincent, Isabelle Louveau, Florence Gondret, Christine Trefeu, Hélène Gilbert, Louis Lefaucheur

Published June 25, 2015

Divergent selection for residual feed intake affects the transcriptomic and proteomic profiles of pig skeletal muscle[1,2]

A. Vincent,*† I. Louveau,*† F. Gondret,*† C. Tréfeu,*† H. Gilbert,‡§# and L. Lefaucheur*†[3]

*INRA, UMR1348 Pegase, F-35590 Saint-Gilles, France; †Agrocampus Ouest, UMR1348 Pegase, F-35000 Rennes, France; ‡INRA, UMR1388 GenPhySE, F-31326 Castanet-Tolosan, France; §Université de Toulouse, INP, ENSAT, UMR1388 GenPhySE, F-31326 Castanet-Tolosan, France; #Université de Toulouse, INP, ENVT, UMR1388 GenPhySE, F-31076 Toulouse, France

ABSTRACT: Improving feed efficiency is a relevant strategy to reduce feed cost and environmental waste in livestock production. Selection experiments on residual feed intake (RFI), a measure of feed efficiency, previously indicated that low RFI was associated with lower feed intake, similar growth rate, and greater lean meat content compared with high RFI. To gain insights into the molecular mechanisms underlying these differences, 24 Large White females from 2 lines divergently selected for RFI were examined. Pigs from a low-RFI ("efficient") and high-RFI ("inefficient") line were individually fed ad libitum from 67 d of age (27 kg BW) to slaughter at 115 kg BW (n = 8 per group). Additional pigs of the high-RFI line were feed restricted to the daily feed intake of the ad libitum low-RFI pigs (n = 8) to investigate the impact of selection independently of feed intake. Global gene and protein expression profiles were assessed in the LM collected at slaughter. The analyses involved a porcine commercial microarray and 2-dimensional gel electrophoresis. About 1,000 probes were differentially expressed ($P < 0.01$) between RFI lines. Only 10% of those probes were also affected by feed restriction. Gene functional classification indicated a greater expression of genes involved in protein synthesis and a lower expression of genes associated with mitochondrial energy metabolism in the low-RFI pigs compared with the high-RFI pigs. At the protein level, 11 unique identified proteins exhibited a differential abundance ($P < 0.05$) between RFI lines. Differentially expressed proteins were generally not significantly affected by feed restriction. Mitochondrial oxidative proteins such as aconitase hydratase, ATP synthase subunit α, and creatine kinase S-type had a lower abundance in the low-RFI pigs, whereas fructose-biphosphate aldolase A and glyceraldehyde-3-phosphate dehydrogenase, 2 proteins involved in glycolysis, had a greater abundance in those pigs compared with high-RFI pigs. Antioxidant proteins such as superoxide dismutase and glutathione peroxidase 3 at the mRNA level and peroxiredoxin-6 at the protein level were also less expressed in LM of the most efficient pigs, likely related to lower oxidative molecule production. Collectively, both the transcriptomic and proteomic approaches revealed a lower oxidative metabolism in muscle of the low-RFI pigs and all these modifications were largely independent of differences in feed intake.

Key words: feed efficiency, muscle, pig, proteome, transcriptome

 J. Anim. Sci. 2015.93:2745–2758
doi:10.2527/jas2015-8928

[1]The authors would like to thank M. Alix, R. Janvier, J. Liger, V. Piedvache, P. Roger, and J. F. Rouault for their involvement in animal care and slaughtering and P. Ecolan and S. Tacher for their help in tissue sampling and expert technical assistance. We are also grateful to Y. Billon and A. Priet for providing divergently selected piglets. F. Moreews from the Sigenae team is acknowledged for updating the Agilent microarray annotation and thanks are also due to the Proteomics Core Facility at Biogenouest (Rennes, France) for protein spot identification.

[2]The study was financially supported by the French National Research Agency (Agence Nationale de la Recherche, ANR-08-GENM038, PIG_FEED project).

[3]Corresponding author: Louis.Lefaucheur@rennes.inra.fr

Received January 16, 2015.
Accepted April 6, 2015.

INTRODUCTION

Improving feed efficiency is a major objective in livestock production to reduce feed cost and environmental waste. Feed efficiency can be assessed by estimating residual feed intake (**RFI**) of growing animals, defined as the feed consumed above or below what is predicted for growth and maintenance. Therefore, animals with low RFI (**RFI$^-$**) consume less feed than predicted and are qualified as efficient animals. In pigs, selection experiments have shown that reduced RFI is genetically correlated with lower feed intake and a leaner carcass, without any marked effects on growth rate (Gilbert et al., 2007). In skeletal muscle, larger fast-twitch glycolytic fibers with higher glycogen content and a greater proportion of glycolytic fibers have been reported in RFI$^-$ pigs compared with high RFI (**RFI$^+$**) pigs (Lefaucheur et al., 2011). In addition, lower activities of some glycolytic and oxidative enzymes have been reported in muscle of RFI$^-$ pigs (Le Naou et al., 2012; Faure et al., 2013), suggesting differences in muscle metabolic orientations for the storage and use of nutrients between lines. In cattle, differences in tissue metabolism have also been shown to contribute to differences in feed efficiency (Richardson and Herd, 2004). Nevertheless, the underlying biological basis of these differences remains to be fully established.

During the last decade, high-throughput technologies such as transcriptomics and proteomics have been used for large-scale genome expression analysis. These technologies may allow the identification of genes, proteins, or biological pathways that were not described so far to be responsive to the divergent selection for RFI. Therefore, this study aimed to investigate global modifications in gene and protein expressions in skeletal muscle between 2 pig lines divergently selected for RFI. Direct effects of RFI divergence on metabolic orientation was discriminated from the selection-induced differences in feed intake by considering an additional pair-fed RFI$^+$ group.

MATERIALS AND METHODS

Animals

The care and use of pigs were performed in compliance with the European Union legislation (directive 86/609/CEE; http://ec.europa.eu/food/fs/aw/aw_legislation/scientific/86-609-eec_fr.pdf; accessed 27 January 2009) and the French legislation (Décret number 2001-464 29/05/01; http://ethique.ipbs.fr/sdv/charteexpeanimale.pdf [accessed 29 January 2009]; agreement for animal housing number C-35-27532). Moreover, the technical and scientific staff involved in the experiment got an individual agreement from the French Veterinary Services to experiment on living animals. As previously described (Gilbert et al., 2007), ADFI and ADG from 35 to 95 kg were recorded on male candidates to selection, together with live backfat thickness at 95 kg BW. An RFI selection index was computed as a linear combination of those traits to account for growth requirements, with variations of maintenance requirements being ignored between fixed BW. In the present study, pigs from the seventh and eighth generations of divergent selection were considered. Average breeding values for RFI in those pigs were 57.6 and –70.7 g/d for the high-RFI RFI$^+$and RFI$^-$ line, respectively, which were not different from the average breeding values calculated in these generations for sibs bred.

Purebred French Large White female pigs in the course of a divergent selection experiment for RFI were produced at the INRA research farms (GenESI at Surgères, Rouillé and Le Magneraud, France). This study was part of a larger contemporary work whose results related to performance, body composition, tissue energy metabolism, and hormonal status have already been published (Le Naou et al., 2012). Briefly, female piglets from the RFI$^-$ (n = 8) and RFI$^+$ (n = 16) lines considered in the present study were weaned at 28 d of age and immediately transferred to the experimental facilities of INRA Pegase (Saint-Gilles, France). They were housed in collective pens (1 pen per line) at arrival and had free access to feed. At 67 ± 1 d of age, pigs were individually housed up to commercial slaughter BW of 115 kg. Pigs had free access to a transition diet the first week and were then divided into 3 experimental groups. In the first group, the RFI$^-$ pigs were fed ad libitum (RFI$^-$; n = 8). Littermates of the RFI$^+$ line were divided into 2 experimental groups having either free access to feed (RFI$^+$; n = 8) or receiving the same amount of feed per metabolic BW ($BW^{0.60}$) as RFI$^-$ pigs (feed-restricted RFI$^+$ pigs [**RFI^{+R}**]; n = 8). Pigs were weighed weekly and feed consumption was recorded daily. Daily feed allocated to RFI^{+R} pigs was calculated weekly, based on the average daily feed consumption recorded during the week before in RFI$^-$ group, the average BW of RFI$^-$ and RFI^{+R} pigs at the day of calculation, and the predicted ADG of RFI$^-$ pigs for the week after.

Animals had free access to water and were fed with standard diets formulated for postweaning and growing periods as previously described (Le Naou et al., 2012). Pigs were weighed weekly and on slaughter day. Feed consumption (feed offered minus refusals) was recorded daily throughout the experiment.

Animal Slaughtering and Sample Collection

Pigs were slaughtered at 115.2 ± 1.5 kg BW by electronarcosis followed by exsanguination 2 h after their first morning meal, at the experimental slaughterhouse of INRA (Saint-Gilles, France). Samples of LM were collected at the last rib level within 20 min after death, cut into small pieces, snap frozen in liquid nitrogen, and stored at –75°C until further analyses.

Ribonucleic Acid Extraction

For total RNA extraction, 80 to 100 mg of frozen muscle was homogenized in Trizol reagent (Invitrogen, Cergy-Pontoise, France) using a TissueLyser (Qiagen, Hilden, Germany) and was then treated as previously described (Vincent et al., 2012). The RNA was purified using a silica-membrane technology under vacuum (Nucleospin 8 RNA kit; Macherey Nagel, Hoerdt, France). The quantification of RNA was performed by using a NanoDrop ND-1000 spectrophotometer (Thermo Scientific, Illkirch, France). Ratios of A260:A280 and A260:A230 were greater than 1.8 in all samples, denoting good purity. The integrity of total RNA was assessed using the Agilent RNA 6000 Nano kit with an Agilent 2100 Bioanalyzer (Agilent Technologies France, Massy, France). Average RNA integrity numbers were 8.1 ± 0.5 (mean ± SD).

Microarray Analysis

Transcriptomics analyses were performed using the porcine commercial Agilent-026440 Oligo Microarray (V2, 4x44K, GPL15007; Agilent Technologies France), containing 43,803 probes. To update annotation of the porcine gene chip probe sets, Agilent 60-mer probes were further analyzed on the basis of probe and contig sequence homology searches using pig transcripts (National Center for Biotechnology Information [**NCBI**] *Sus scrofa* RefSeq; http://www.ncbi.nlm.nih.gov/RefSeq/ [accessed 5 March 2012]; UniProt; http://www.uniprot.org/ [accessed 8 March 2012]) or transcripts from related species (*Homo sapiens*, *Bos taurus*, and *Mus musculus*). Annotation was based on similarity and quality criteria as follows: at least 18 consecutive base pairs within the 60-mer probe sequence and 85% homology (Casel et al., 2009). In total, 33,231 probes (76% of total) were annotated, corresponding to 12,332 unique gene symbols.

Each sample was labeled with Cy3 dye using the Low RNA Input Linear Amplification Kit (Agilent Technologies France) following the manufacturer's instructions. Briefly, a 2-step procedure was used to generate fluorescent complementary RNA by using T7 RNA polymerase. Samples were then purified with an RNeasy MinElute kit (Qiagen). Microarray hybridizations were performed in Agilent's SureHyb hybridization chambers containing 1.65 µg of Cy3-labeled complementary RNA sample per hybridization. Hybridization reactions were performed at 65°C for 17 h using Agilent's Gene Expression Hybridization kit. After washing, microarrays were scanned at 5 µm/pixel resolution using the Agilent DNA Microarray Scanner G2505C, and images were analyzed with Agilent Feature Extraction Software (version 10.7.3.1; protocol GE1_107_Sep09). All analyses were then performed using the R software version 2.10.0 (R Development Core Team, 2008). Raw spot intensities were first submitted to quality filtration based on 4 criteria: intensity, uniformity, saturation, and outliers detection. Among the 43,803 probes evaluated per microarray, 29,364 probes (67%) were kept after quality filtration. Intensities of filtered spots were log2 transformed, and data were normalized by median centering, that is, subtracting the median value across all probes from all raw values within each sample. Microarray selected data have been deposited into the Gene Expression Omnibus repository and are publicly available through Gene Expression Omnibus accession number GSE47769 (http://www.ncbi.nlm.nih.gov/geo/query/acc.cgi?acc=GSE47769; accessed 10 June 2013). Data were then submitted to ANOVA using the fixed effects of the genetic line (RFI^- or RFI^+) or feed restriction (RFI^{+R} or RFI^+). Differentially expressed (**DE**) probes with *P*-values lower than 0.01 were then selected for further functional analysis.

Functional Analysis

Probes that were DE between RFI^- and RFI^+ pigs were then divided into down- or upregulated probes. These 2 lists of probes were further investigated by an enrichment analysis of specific Gene Ontology (**GO**) terms for Biological Processes and Kyoto Encyclopedia Genes and Genomes pathways using the Database for Annotation, Visualization and Integrated Discovery (**DAVID**) bioinformatic resources (http://david.abcc.ncifcrf.gov/home.jsp; accessed 10 April 2012; Huang. et al., 2008; Dennis et al., 2003). In DAVID analysis, the GO terms_FAT were selected to filter the broadest terms without overshadowing the more specific ones. The lists of probes were uploaded using official gene symbol obtained with DAVID Gene Acession Conversion Tool. The *P*-values for enrichment were computed by a modified Fisher's exact test, using the porcine microarray as the background. The REVIGO Web server (http://revigo.irb.hr/; accessed 4 February 2013) was also used to reduce redundancy and to find the most representative GO terms (Supek et al., 2011).

The SimRel was used as the semantic similarity measure within the human GO database (Schlicker et al., 2006). Tables were chosen to visualize the results.

Proteome Analysis

Total proteins were extracted from 50 mg of powdered frozen muscle tissue homogenized into 1 mL lysis buffer containing 7.5 *M* urea, 2 *M* thiourea, 2% 3-((3-cholamidopropyl)dimethylammonium)-1-propanesulfonate, 40 m*M* Tris base, 50 m*M* dithiothreitol (**DTT**), 1 m*M* EDTA, 1% immobilized pH gradient (**IPG**) buffer pH 3 to 11 nonlinear (**NL**; GE Healthcare, Uppsala, Sweden), 1 µg/mL pepstatin, and 1.5 mg/mL complete protease inhibitor cocktail (Roche, Mannheim, Germany), using a handheld Teflon-pestle-glass Potter-Elvehjem homogenizer. The lysate was incubated at room temperature for 1 h with rotational shaking followed by centrifugation at 60,000 × *g* for 1 h at 18°C. Supernatant was collected avoiding the fat layer, aliquoted, and stored at –75°C until further analysis. Protein concentration in the supernatants was determined using the Quick Start Bradford kit (Bio-Rad, Marnes-la-Coquette, France) with BSA as the standard. For the first dimension electrophoresis, 300 µg protein was diluted in a rehydration buffer containing 0.5% IPG buffer pH 3 to 11 NL and Destreack solution (GE Healthcare) to a final volume of 450 µL. Precast NL immobilized gradient strips (pH 3–11, 24 cm; GE Healthcare) were rehydrated overnight (16 h) at room temperature in a passive way with the solubilized proteins under 3.5 mL of cover fluid (GE Healthcare). The IPG strips were then subjected to isoelectric focusing on an Ettan IPGphorII system (GE Healthcare) at 20°C with a step gradient protocol ranging from 150 to 8,000 V for 21 h (150 V for 1 h, 300 V for 3 h, 300 to 600 V for 1 h, 600 to 1,000 V for 4 h 30 min, 1,000 to 8,000 V for 3 h, and 8,000 V for 8 h 45 min) to reach a total of 88,600 V·h. At the completion of focusing, the strips were equilibrated by soaking for 15 min in 50 m*M* Tris-HCl buffer pH 8.8, 6 *M* urea, 30% glycerol, 2% SDS, and 65 m*M* DTT followed by an additional 15 min equilibration in the same buffer replacing DTT by 4.5% iodoacetamide and adding 0.03% bromophenol blue sodium salt R-250 (Sigma -Aldrich, Saint-Quentin Fallavier, France). Equilibrated IPG strips were transferred onto the top of a 12.5% uniform SDS-PAGE and sealed with 0.5% (wt/vol) low-melting-point agarose. The SDS-PAGE was performed in a vertical Ettan DALTsix system (GE Healthcare) using upper 2x and lower 1x buffer (number 161-0772; Bio-Rad) at 15°C. Gels were run at 5 W/gel for 45 min followed by 17 W/gel until bromophenol blue front reached the bottom of the gel. After migration, gels were fixed overnight in 40% methanol/10% acetic acid, rinsed 3 times for 5 min in water, and stained by 0.12% Coomasie Brilliant Blue G-250 (Bio-Rad) in 10% phosphoric acid, 10% ammonium sulfate, and 20% methanol for 24 h. Following destaining in water, gels were scanned using an UMAX ImageScanner (GE Healthcare) at 300 dots per inch and spot detection and quantification were performed by image analysis (Melanie 2D gel analysis software version 7.0; SIB Swiss Institute of Bioinformatics, Lausanne, Switzerland). To take into account experimental variation (protein loading and staining), 2-dimensional (**2D**) gels were normalized within each gel by dividing each spot volume by the total volume of all valid spots on the gel (spot relative volume expressed as vol/vol × 10^6). Highly abundant protein spots such as actin were manually deleted because of inaccurate quantification due to saturation. Data were then analyzed by ANOVA using the GLM procedure of SAS (SAS Inst. Inc., Cary, NC) with the fixed effect of the experimental group (RFI^-, RFI^+, and RFI^{+R}). A *P*-value lower than 0.05 was retained for statistical significance.

Preparative gels with 600 µg of proteins from pooled samples were performed for spot picking. The protein spots that were different between RFI^- and RFI^+ pigs were punched out of preparative gels using a OneTouch 2D gel manual spotpicker (Gel Company, San Francisco, CA). In gel tryptic digestion and protein identification by mass spectrometry were performed in the high-core proteomic facilities of Biogenouest (Rennes, France) as previously described (Colinet et al., 2012). Briefly, tryptic peptides were analyzed by nano–liquid chromatography-tandem mass spectrometry **(LC-MS/MS)** using nano–liquid chromatography system Ultimate 3000 (DIONEX; LC Packings, Amsterdam, The Netherlands) coupled online to a linear ion trap HCT Ultra P Discovery system mass spectrometer (BrukerDaltoniK GmBh, Bremen, Germany). The proteinScape 2.1 software (BrukerDaltoniK GmBh) was used to submit tandem mass spectrometry data to the following database: SwissProt sequence database restricted to mammalia taxonomy (http://www.uniprot.org; accessed 9 October 2012) and NCBI nonredundant sequences databases of mammalian proteins (http://www.ncbi.nlm.nih.gov; accessed 9 October 2012) using the Mascot search engine (Mascot server version 2.2; http://www.matrixscience.com; accessed 9 October 2012). Parameters were set as follows: trypsin as enzyme with one allowed miscleavage, carbamidomethylation of cysteins as fixed modification, and methionine oxidation as variable modifications. The mass tolerance for parent and fragment ions was set to 1.2 and 0.5 Da,

respectively. Results were scored using the probability-based Mowse algorithm, where the protein score is $-10 \times \log(P)$ and P is the probability that the observed match is a random event. In our conditions, a score greater than 80 indicated a significant identification ($P < 0.05$) and at least 4 matched peptides per protein and 20% sequence coverage were also required to avoid incorrect identification. The accuracy of the experimental to theoretical isoelectric point and molecular weight were also considered. Identified proteins were then classified according to their biological process terms provided in GO Consortium for *Homo sapiens* by using correspondence to gene name and their functions proposed on the SwissProt/TrEMBL protein databases (http://www.uniprot.org/; accessed 25 October 2012).

Quantitative Real-Time PCR

Expressions of selected genes found to be DE between RFI lines by transcriptome and proteome analyses or by transcriptome analysis only were further evaluated by quantitative real-time PCR (**qPCR**). Complementary DNA was synthesized from 1 μg of total RNA previously used in microarray analysis, using a High Capacity cDNA Reverse Transcription Kit (Applied Biosystems, Foster City, CA). Primers (Table 1) were designed from porcine sequences using Primer Express software 3.0 (Applied Biosystems). For each primer pair, the amplification efficiency of qPCR reaction was determined using calibration curves generated with 6 decreasing concentrations of cDNA from pooled muscle samples (obtained from 12.5 to 12.5×10^{-3} ng RNA). Amplification reaction was performed in duplicate in 12.5 μL with 2.5 ng of reverse-transcribed RNA and both forward and reverse primers (200 n*M* each) in 1x PCR buffer (Fast SYBR Green Master Mix; Applied Biosystems). A StepOnePlus Real Time PCR system (Applied Biosystems) was used. Thermal cycling conditions were as follows: 50°C for 2 min and 95°C for 20 s followed by 40 cycles of denaturation at 95°C for 3 s and annealing at 60°C for 30 s. Specificity of the amplification products was checked by dissociation curves analysis. Three genes were found invariant and, therefore, used as reference for normalization according to the geNorm algorithm (Vandesompele et al., 2002): *hypoxanthine phosphoribosyltransferase 1* (*HPRT1*), *peptidylpropyl isomerase A (cyclophilin A)* (*PPIA*), and *tyrosine 3-monooxygenase/tryptophan 5-monooxygenase activation protein, zeta polypeptide* (*YWHAZ*). For each sample, a normalization factor (**NF**) was calculated using the geNorm algorithm and used for subsequent normalization. For each gene, the normalized expression level N was calculated according to the following formula (Pfaffl, 2001): $N = E^{-\Delta Cq_{(sample\ -\ calibrator)}}/NF$, in which E is calculated from the slope of calibration curve, Cq is the quantification cycle, and calibrator is a pool of all muscle samples. Data were analyzed by ANOVA with the fixed effect of genetic line by using the R software version 2.10.0 (R Development Core Team, 2008). A P-value < 0.05 was retained for statistical significance.

RESULTS

Residual Feed Intake and Feed Restriction Effects on Performance

The RFI^- and RFI^{+R} pigs were older (+10 to 13 d; $P < 0.001$) than RFI^+ pigs at the same slaughter BW (Table 2). From 67 d of age to slaughter, ADG did not differ between RFI^- and RFI^+ pigs and was lower in RFI^{+R} pigs (–10%). Daily feed intake was similar in RFI^- and RFI^{+R} pigs ($P > 0.05$), whereas ADFI was markedly lower ($P < 0.001$) in these groups compared with RFI^+ pigs when adjusted to metabolic BW (182, 181, and 209 $g \cdot d^{-1} \cdot kg^{-1}$ $BW^{0.60}$ in RFI^-, RFI^{+R}, and RFI^+ pigs, respectively) or calculated on an as-fed basis (2.23, 2.32 and 2.65 kg/d, respectively). The G:F was greater ($P < 0.001$) in RFI^- than RFI^+ pigs. Feed restriction in RFI^{+R} was rather moderate (–13% on a metabolic BW basis), so that RFI^{+R} pigs exhibited the same G:F as RFI^+ pigs (0.35). Carcass lean meat content tended to be greater ($P = 0.08$) in RFI^- and RFI^{+R} pigs than in RFI^+ pigs.

Residual Feed Intake and Feed Restriction Effects on Muscle Transcriptome

In muscle, 1,013 probes were DE between RFI^- and RFI^+ pigs ($P < 0.01$) with 82% of them exhibiting a fold change below the absolute value of 1.5 (Table 3). Among these probes, 674 (corresponding to 338 annotated genes) were overexpressed and 339 (corresponding to 188 annotated genes) were underexpressed in RFI^- pigs compared with RFI^+ pigs. The number of DE probes ($P < 0.01$) between RFI^+ and RFI^{+R} pigs was lower (727) than the number of DE probes between RFI^- and RFI^+ pigs. Among them, 402 probes were overexpressed in RFI^{+R} pigs compared with RFI^+ pigs. Only 53 of these probes were also found to be overexpressed in RFI^- vs. RFI^+ pigs. Among the 325 probes downregulated in RFI^{+R} pigs compared with RFI^+ pigs, only 37 were also downregulated in RFI^- vs. RFI^+ pigs. Therefore, only 10% of the DE probes between RFI lines were also affected by feed restriction. Therefore, the functional analysis

Table 1. Primer sequences used for analysis of gene expression by quantitative real-time PCR

Gene symbol	Description	Accession number[1]	Primer sequence (5′–3′)[2]
AQP4	*Aquaporin 4*	ENSSSCT00000004120	F: CAGAAAAGCCCCTACCTGTTGA R: CGTGACAGCGGGATTGATG
CD40	*CD40 molecule, tumor necrosis factor receptor superfamily member 5*	ENSSSCT00000008144	F: GCCCGCCAGGACAGAAA R: GGAACTGCAAGGAAGGCATTC
CSRNP3	*Cysteine-serine-rich nuclear protein 3*	ENSSSCT00000017319	F: TCAATCCATCCACTTCCAATCA R: GCCGCTTCTCCCTTTTGAG
GAPDH	*Glyceraldehyde-3-phosphate dehydrogenase*	AF017079.1	F: CATCCATGACAACTTCGGCA R: GCATGGACTGTGGTCATGAGTC
GPX3	*Glutathione peroxidase 3*	ENSSSCT00000018610	F: GCTTCCCCTGCAACCAATT R: GGACATACCTGAGAGTGGACAGAA
OAZ3	*Ornithine decarboxylase antizyme 3*	NM_001122996	F: ATTGTATTCGGCTGGGAACCT R: GGCGGAAGTGGAAGTCTAGCT
PCIF1	*Phosphorylated CTD-interacting factor 1*	XM_003360023	F: CAGCGTGGAGATGCACATG R: GAGCCACAGCTTGCTGAAGTAG
PRMT3	*Protein arginine methyltransferase 3*	XM_003360703	F: CAGGTGAAGGCTTGAAAGGAA R: TCACAATGAGAGAACGTGGATCTT
SOD2	*Superoxide dismutase 2, mitochondrial*	NM_214127.2	F: GCGCTGAAAAAGGGTGATGT R: ACCGTTAGGGCTCAGATTTGTC
WDHD1	*WD repeat and HMGbox DNA binding protein 1*	ENSSSCT00000005569	F: GCCATTCCAGTCAGGTTCTACAC R: TCCAATAGAATTCCACACCATGAA
HPRT1[3]	*Hypoxanthine phospho-ribosyltransferase 1*	DQ845175	F: TACCTAATCATTATGCCGAGGATTT R: AGCCGTTCAGTCCTGTCCAT
PPIA[3]	*Peptidylpropyl isomerase A*	NM_214353	F: AGCACTGGGGAGAAAGGATT R: AAAACTGGGAACCGTTTGTG
YWHAZ[3]	*Tyrosine 3-mono-oxygenase/tryptophan 5-monooxugenase activation protein, zeta polypeptide*	XM_001927228	F: ATGCAACCAACACATCCTATC R: GCATTATTAGCGTGCTGTCTT

[1]Accession number in the National Center for Biotechnology Information database (http://www.ncbi.nlm.nih.gov/gene; accessed 14 May 2013) or Ensembl project database (http://www.ensembl.org/Sus_scrofa/Info/Index; accessed 14 May 2013) for pig sequences.

[2]F = forward primer; R = reverse primer.

[3]Genes used as reference for quantitative real-time PCR normalization.

was further focused on the effects of genetic differences between RFI lines.

Functional analysis of DE genes between RFI^- and RFI^+ groups showed an overrepresentation of pathways related to oxido-reduction process and energy oxidative metabolism in RFI^+ pigs (Table 4). Especially, the expression levels of genes encoding *glutathione peroxidase 3* (*GPX3*) and *superoxide dismutase 2* (*SOD2*), 2 enzymes involved in the detoxification of reactive oxygen species (**ROS**), were lower in RFI^- than in RFI^+ pigs. Moreover, many genes involved in the respiratory electron transport chain, the generation of precursor metabolites and energy, and the tricarboxylic acid cycle were downregulated in RFI^- pigs compared with RFI^+ pigs (Table 4). This concerned the expression of genes encoding mitochondrial *NADH dehydrogenase 1* (*ND1*), *2* (*ND2*), and *4* (*ND4*); *NADH dehydrogenase* (*ubiquinone*) *1 β subcomplex 9* (*NDUFB9*); *isocitrate dehydrogenase* 3 (*NAD+*) *α* (*IDH3A*); and *cytochrome C* (*CYCS*; Table 4). *Electron-transfer-flavoprotein beta polypeptide* (*ETFB*), which serves as a specific electron acceptor for several acyl-CoA dehydrogenases and transfers the electrons to the mitochondrial respiratory chain via electron-transferring-flavoprotein dehydrogenase, was also underexpressed in RFI^- pigs. However, other functionally important genes might have been missed because they did not fit into a cluster. Therefore, additional individual DE genes were also taken into account to extend the global functional analysis (Table 5). *Dihydrolipoamide dehydrogenase* (*DLD*) and *pyruvate dehydrogenase kinase isozyme 1* (*PDK1*), 2 genes involved in mitochondrial pyruvate metabolism, were found to be underexpressed in RFI^- pigs. *Acyl-CoA thioesterase 8* (*ACOT8*) and *lipase A* (*LIPA*), coding for proteins involved in acyl-CoA hydrolysis and lipase activity, respectively, were also underexpressed in RFI^- pigs compared with RFI^+ pigs. *Vascular endothelial growth factor A* (*VEGFA*), a gene coding for a growth factor active in angiogenesis and vasculogenesis, was also notably underexpressed in RFI^- pigs. The expressions of 2 other genes related to apotosis, *CSRNP3* (i.e., a transcriptional factor involved in apoptosis) and *OAZ3*, an inhibitor of ornithine decarboxylase, which is an enzyme involved in the antioxidative defense and resistance to apoptosis through the generation of polyamines, were also expressed at lower levels in RFI^- pigs (Table 5). Finally,

Table 2. Growth performance and carcass traits in pigs divergently selected for low (RFI$^-$) or high (RFI$^+$) residual feed intake (RFI) having either free (RFI$^-$ and RFI$^+$) or restricted (RFI^{+R}) access to feed from 67 d of age to slaughter. Values are least squares means

Item	RFI$^-$ (n = 8)	RFI$^+$ (n = 8)	RFI^{+R} (n = 8)	RSD[1]	P-value
Growth traits					
67-d-old BW, kg	25.7[b]	31.1[a]	30.5[a]	3.9	0.02
Final BW, kg	115.8	114.9	115.2	1.6	0.51
Final age, d	168[a]	158[b]	172[a]	6.23	<0.001
ADG, g/d	892[a]	927[a]	819[b]	39	<0.001
Feed intake					
Daily feed intake, g·d^{-1}·kg BW$^{0.60}$	182[a]	209[b]	181[a]	10	<0.001
G:F	0.40[a]	0.35[b]	0.35[b]	0.02	<0.001
Carcass traits					
Lean meat content, %	59.0	57.2	58.9	2.0	0.08

[a,b]Within a row, means without a common superscript differ (P < 0.10).

[1]RSD = residual SD (corresponding to the root-mean-square error of the full ANOVA model).

genes associated with antigen processing and presentation of peptide antigen and endosome transport, such as *HLA-A*, *HLA-B*, and *HLA-C*, were downregulated in RFI$^-$ pigs (Table 4). Functional analysis of upregulated genes in RFI^{+R} pigs compared with RFI$^+$ pigs reveals significant enrichments of GO terms associated with RNA processing, intracellular protein transport, and ubiquitin-dependent protein catabolic processes.

Conversely, translation biological processes such as translation itself, ribonucleoprotein complexes, and mRNA processing were upregulated pathways in RFI$^-$ vs. RFI$^+$ pigs (Table 4). In particular, genes coding for translation initiation and elongation factors (*EEF1A1*, *EEF1G*, *EIF2B5*, *EIF2S2*, and *EIF6*) and RNA processing (*WDHD1*, *POP4*, *CPSF1*, and *CPSF3*) were overexpressed in RFI$^-$ vs. RFI$^+$ pigs (Table 5). *CAPN2*, coding for the millimolar-calpain, a calcium-sensitive cysteine protease, was also overexpressed in RFI$^-$ pigs. Finally, expression level of the *glyceraldehyde-3-phosphate dehydrogenase* (*GAPDH*), a metabolic enzyme involved in the glycolytic pathway, was greater in RFI$^-$ pigs than in RFI$^+$ pigs (Table 5).

Residual Feed Intake and Feed Restriction Effects on Muscle Proteome

About 807 spots were detected and matched between the 24 gels (Fig. 1). Among them, 20 spots were found with a differential abundance between RFI$^-$ and RFI$^+$ pigs (P < 0.05) and 15 spots were less intense in RFI$^-$ pigs compared with RFI$^+$ pigs. Fourteen spots, corresponding to 11 unique proteins, were successfully identified (Table 6). Three proteins, each resolved as double spots exhibiting similar molecular weights but different isoelectric points (Fig. 1), corresponded to ATP synthase subunit α (ATP5A1), creatine kinase S-type (CKMT2), and heat shock protein β-1 (HSPB1). Differences between RFI$^-$ and RFI$^+$ pigs were similar between double spots for ATP5A1**,** and CKMT2 and opposite for HSPB1. The 11 identified proteins could be divided into 4 different functional groups: metabolism related (6 proteins), stress related (2 proteins), transport related (2 proteins), and structure related (1 protein; Table 6). Among the metabolism-related proteins, 3 were related to mitochondrial oxidative metabolism (ACO2, ATP5A1, and CKMT2) and were less abundant in RFI$^-$ than RFI$^+$ animals (P < 0.05). The stress-related protein peroxiredoxin-6 (PRDX6), involved in protection against oxidative stress, was decreased (P < 0.05) in RFI$^-$ animals compared with RFI$^+$ animals and was downregulated by feed restriction, so that RFI^{+R} pigs and RFI$^-$ pigs did not differ. The cytoplasmic glycerol-3-phosphate dehydrogenase (GPD1), an enzyme involved in the glycerol phosphate shuttle, was also less abundant in RFI$^-$ than RFI$^+$ animals. Conversely, 2 proteins related with glycolytic metabolism (GAPDH and fructose-bisphosphate aldolase A [ALDOA]) had a greater abundance in RFI$^-$ than RFI$^+$ pigs. These metabolism-related proteins were not influenced by feed restriction in the RFI$^+$ pigs. Among transport related proteins, serotransferrin (TF), a secreted protein involved in iron transport, and myoglobin (MB) involved in oxygen transport within myofibers were less abundant in RFI$^-$ pigs compared with RFI$^+$ pigs (P < 0.05). Relative abundance of myoglobin was not significantly influenced by feed restriction, whereas abundance of TF protein was lower in RFI^{+R} vs. RFI$^+$ pigs (P < 0.05). Finally, vascular smooth muscle actin (ACTA2), a structure-related protein, was identified as having a lower abundance in RFI$^-$ than RFI$^+$ animals

Table 3. Number of probes differentially expressed (P < 0.01) in muscle of pigs divergently selected for low (RFI$^-$) or high (RFI$^+$) residual feed intake (RFI) having either free (RFI$^-$ and RFI$^+$) or restricted (RFI^{+R}) access to feed from 67 d of age to slaughter at 115 kg BW

	RFI$^-$/RFI$^+$ pigs		RFI^{+R}/RFI$^+$ pigs	
Fold-change groups	Over-expressed	Under-expressed	Over-expressed	Under-expressed
Total	674	339	402	325
FC[1] ≥ 1.5	72	110	18	80
FC ≥ 2	27	32	1	3

[1]FC = fold change.

Table 4. Most significant overrepresented Gene Ontology (GO) biological processes identified from the differentially expressed genes between muscles of low (RFI$^-$) and high (RFI$^+$) residual feed intake pigs having free access to feed from 67 d of age to slaughter

GO accession	Description	No.[1]	Log10 *P*-value	Gene symbol
Downregulated in RFI$^-$ vs. RFI$^+$				
GO:0055114	Oxidation-reduction process	19	–4.243	*ME1*, *ND1*, *ND4*, *LOC396756*, *NDUFB9*, *ND2*, *CYCS*, *MOSC2*, *IDH3A*, *SOD2*, *RDH11*, *SLC1A3*, *HSDL2*, *FMO1*, *GPX3*, *DLD*, *HSD17B4*, *LOC733694*, and *ETFB*
GO:0048002	Antigen processing and presentation of peptide antigen	5	–3.958	*SLA-3*, *HLA-A*, *HLA-C*, *HLA-B*, and *B2M*
GO:0022900	Electron transport chain	8	–3.696	*ND1*, *SLC1A3*, *ND4*, *LOC396756*, *NDUFB9*, *ND2*, *CYCS*, and *ETFB*
GO:0006091	Generation of precursor metabolites and energy	10	–2.248	*ND1*, *SLC1A3*, *ND4*, *LOC396756*, *PGAM4*, *NDUFB9*, *ND2*, *CYCS*, *ETFB*, and *IDH3A*
GO:0016197	Endosome transport	4	–1.614	*STX16*, *PIKFYVE*, *VPS13A*, and *HOOK3*
GO:0045944	Positive regulation of transcription from RNA polymerase II promoter	8	–1.327	*TAF2*, *CSRNP3*, *MITF*, *SIX1*, *CAND1*, *TCEA1*, *TCF7L2*, and *STAT3*
Upregulated in RFI$^-$ vs. RFI$^+$				
GO:0006412	Translation	37	–23.118	*EIF6*, *RPL18*, *RPL14*, *RPLP0*, *RPLP1*, *FAU*, *RPL10*, *RPL12*, *RPL36AL*, *EIF2B5*, *LOC645139*, *RPS18*, *RPS19*, *RPS12*, *UBA52*, *RPS26*, *RPL7*, *RPL6*, *RPL8*, *RPS20*, *RPS23*, *RPSA*, *EEF1A1*, *PAIP1*, *RPL23A*, *DENR*, *RPS6*, *COPS5*, *LOC100049695*, *RPS19P3*, *RPS3*, *EEF1G*, *RPS15A*, *RPL29*, *RPL23*, *RPL21*, and *EIF2S2*
GO:0022613	Ribonucleoprotein complex biogenesis	12	–3.690	*EIF6*, *GTPBP4*, *SNUPN*, *LOC100049695*, *GNL3L*, *RPS6*, *SFRS5*, *RPS19*, *RPL7*, *RPLP0*, *POP4*, and *TGS1*
GO:0042692	Muscle cell differentiation	9	–2.918	*SYNE1*, *ACTA1*, *MAPK12*, *ERBB2*, *GLMN*, *SOX6*, *NEURL2*, *CAPN2*, and *CACNA1S*
GO:0006379	Messenger RNA cleavage	3	–1.463	*POP4*, *CPSF3*, and *CPSF1*
GO:0030099	Myeloid cell differentiation	5	–1.4411	*RPS19*, *PSEN1*, *EPB42*, *SOX6*, and *VPS33A*
GO:0006469	Negative regulation of protein kinase activity	4	–1.346	*PSEN1*, *HEXIM2*, *SNX6IGF2*, and *PKIA*

[1]Number of genes involved in the GO term.

($P < 0.05$) and was downregulated by feed restriction (RFI^{+R} pigs < RFI$^+$ pigs; $P < 0.05$).

Data Validation by Quantitative Real-Time PCR

Among the DE proteins, only changes in GAPDH were similarly observed both at the mRNA and protein levels between lines. Other DE proteins (ACO2, ATP5A1, CKMT2, ALDOA, GPD1, MB, TF, PRDX6, and HSPB1) were not DE at the mRNA level.

We checked 10 genes showing high fold change in expression levels between RFI$^-$ and RFI$^+$ pigs and involved in various functional categories: oxidative stress (*GPX3*, *SOD2*, and *OAZ3*), glycolysis (*GAPDH*), immune response (*CD40*), apoptose (*CSRNP3* and *OAZ3*), translation (*PCIF1* and *WDHD1*), protein methylation (*PRMT3*), and water transport (*AQP4*). The differential expressions between RFI$^-$ and RFI$^+$ pigs were confirmed by qPCR (Fig. 2) for all tested genes.

DISCUSSION

The current study enriches our knowledge on the molecular mechanisms underlying variations in RFI in pigs selected from a larger group of pigs (Le Naou et al., 2012) by focusing on skeletal muscle transcriptomic and proteomic profiles. To discriminate selection effects from those induced by differences in feed intake, some pigs from the RFI$^+$ line were pair fed at the feeding level of pigs from the RFI$^-$ line during the growing–finishing period. Although Lkhagvadorj et al. (2010) found important effects of an acute caloric restriction on the adipose tissue and liver transcriptomes of pigs divergently selected for RFI, the present study revealed only minor changes in muscle adaptive responses to feed restriction. This discrepancy between our study and the abovementioned one can be related to the organ, variations in experiment duration (several weeks vs. 8 d, respectively), and/or level of feed restriction (13 vs. 75%, respectively). Because only 10% of the DE probes between RFI$^-$ and RFI$^+$ groups were also affected by feed restriction within the RFI$^+$ pigs, our data show that effects of divergent selection for RFI on molecular features of skeletal muscle were quite independent of differences in pig voluntary feed intake between lines.

Table 5. Fold change between the most relevant genes in different biological pathways found between muscles of low (RFI$^-$) and high (RFI$^+$) residual feed intake pigs

Gene symbol	*P*-value maximum[1]	RFI$^-$/ RFI^{+2}	Main Gene Ontology (GO) biological process terms
ND1	0.0045	–1.4	GO:0022904 respiratory electron transport chain
ND2	0.0089	–1.3	
ND4	0.0094	–1.2	
NDUFB9	0.0055	–1.8	
CYCS	0.0074	–1.3	
ETFB	0.0009	–1.3	
IDH3A	0.0082	–1.2	GO:0005975 carbohydrate metabolic process
			GO:0006099 tricarboxylic acid cycle
GAPDH	0.0036	1.4	GO:0006006 glucose metabolic process
DLD	0.0090	–1.2	GO:0006090 pyruvate metabolic process
PDK1	0.0027	–1.4	
ACOT8	0.0005	–1.2	GO:0006637 acyl-CoA metabolic process
			GO:0016559 peroxisome fission
LIPA	0.0069	–1.5	GO:0006629 lipid metabolic process
VEGFA	0.0080	–1.5	GO:0001570 vasculogenesis
GPX3	0.0010	–1.5	GO:0006979 response to oxidative stress
SOD2	0.0073	–1.3	
CSRNP3	0.0001	–2.8	GO:0006915 apoptotic process
OAZ3	1.4×10^{-6}	–1.6	GO:0006521 regulation of cellular amino acid metabolic process
			GO:0034641 cellular nitrogen compound metabolic process
EIF2B5	0.0073	1.2	GO:0006413 translational initiation
EIF2S2	0.0041	1.2	
EEF1A1	0.0098	1.3	GO:0006414 translational elongation
EEF1G	0.0066	1.1	
EIF6	0.0087	1.2	GO:0042256 mature ribosome assembly
WDHD1	0.010	1.3	GO:0006396 RNA processing
POP4	0.001	1.6	
CPSF1	0.0057	1.1	
CPSF3	0.0076	1.3	
CAPN2	0.0024	1.3	GO:0006508 proteolysis
			GO:0016540 protein autoprocessing

[1]The highest *P*-value is reported when several probes are differentially expressed for a unique gene.

[2]The smallest value of expression ratio is reported when several probes are differentially expressed for a gene. Ratios are inversed and preceded by a minus sign for values lower than 1.

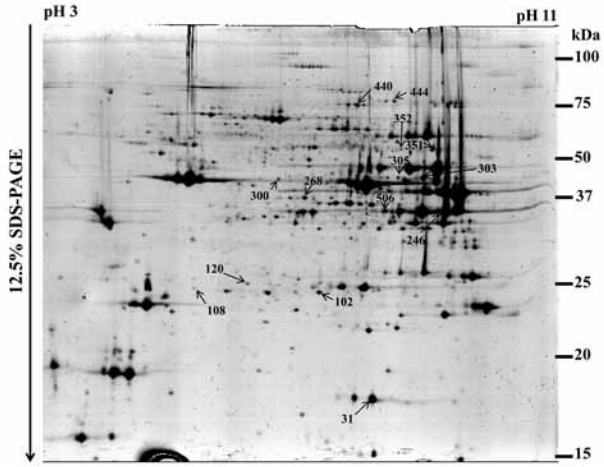

Figure 1. Representative 2-dimensional electrophoresis image of LM separated using an immobilized pH gradient (IPG) 3 to 11 nonlinear strip (GE Healthcare, Uppsala, Sweden) in the first dimension and 12.5% SDS-PAGE in the second dimension. The protein loading was 300 µg and the gel was stained with colloidal Coomassie Brilliant Blue G-250. Numbered spots (14 spots) were identified by nano–liquid chromatography-tandem mass spectrometry (LC-MS/MS) and listed in Table 6.

Lower Muscle Oxidative Metabolism in Low-RFI Pigs

The number of DE mRNA between RFI$^-$ and RFI$^+$ pigs was much greater than the number of differential proteins. These observations likely result from methodological concerns. Indeed, when the microarray technology allows analyses of all spotted genes, an overwhelming number of proteins cannot be detected on 2D gels because their abundance is below the detection threshold. However, common pathways in which individual genes were involved could be found across methodologies. Thus, both transcriptomic and proteomic data indicate that energy metabolism of the predominantly white glycolytic LM was turned to a less oxidative pattern in RFI$^-$ pigs compared with RFI$^+$ pigs. This assumption is supported by the finding of an underexpression in the RFI$^-$ pigs of *dihydrolipoamide dehydrogenase* (*DLD*), a gene that encodes a protein component of the pyruvate dehydrogenase complex regulating the flux of 2-carbon acetyl units from pyruvate through acetyl-CoA into the Krebs cycle and is one of the major enzymes regulating homeostasis of carbohydrate fuels in mammals. This enzyme activity is regulated by a reversible phosphorylation/dephosphorylation cycle by a specific pyruvate dehydrogenase kinase, and the gene encoding the isoform 1 of this protein was also underexpressed in RFI$^-$ pigs. Furthermore, the *IDH3A* gene catalyzing the allosterically regulated rate-limiting step of the tricarboxylic acid cycle was also downregulated in the RFI$^-$ pigs. These findings are further supported by proteomic data showing a lower abundance of aconitase hydratase (ACO2) and ATP synthase subunit α (ATP5A1) in RFI$^-$ pigs. Using a similar gel-based proteome analysis in pig LM, Hwang et al. (2005) identified the same corresponding spots as ACO2 and ATP5A1, which validates the accuracy of spot identification in the present study. The ACO2 catalyzes the isomerization of citrate to isocitrate via *cis*-aconitate in the tricarboxylic acid cycle, whereas ATP5A1 is a subunit of the inner mitochondrial membrane ATP synthase complex (F_0F_1 ATP synthase or Complex V), which produces ATP from ADP in the presence of a proton

Table 6. Differentially expressed muscle proteins in pigs divergently selected for low (RFI$^-$) or high (RFI$^+$) residual feed intake (RFI) having either free (RFI$^-$ and RFI$^+$) or restricted (RFI^{+R}) access to feed from 67 d of age to slaughter

Spot no.[1]	Gene symbol	Protein name[2]	Theoretical pI/Mr[3]	Score[4]	MP/Sc[5]	RFI$^-$: RFI^{+6}	Spot relative volume[7], vol/vol × 10^6			RSD[8]	*P*-value[8]
							RFI$^-$	RFI$^+$	RFI^{+R}		
444	*ACO2*	Aconitase hydratase, mitochondrial	9.0/85.7	1,295	25/25	–1.8	203^a	369^b	343^b	107	0.01
351	*ATP5A1*	ATP synthase subunit α, mitochondrial	9.7/59.7	1,298	29/35	–1.6	683^a	1,060^b	844^{ab}	240	0.02
352	*ATP5A1*	ATP synthase subunit α, mitochondrial	9.7/59.7	932	15/27	–1.6	140^a	219^b	170^{ab}	56	0.03
303	*CKMT2*	Creatine kinase S-type, mitochondrial	9.3/47.2	1,301	29/42	–1.5	995^a	1,527^b	1,322^{ab}	365	0.03
305	*CKMT2*	Creatine kinase S-type, mitochondrial	9.3/47.2	937	12/35	–1.4	240^a	341^b	246^a	78	0.03
506	*GAPDH*	Glyceraldehyde-3-phosphate dehydrogenase	9.3/35.8	732	15/30	1.3	1,563^a	1,184^b	1,410^{ab}	346	0.04
246	*ALDOA*	Fructose-bisphosphate aldolase A	9.2/39.3	1,289	32/42	1.3	26,459^a	21,055^b	22,877^{ab}	3,722	0.03
268	*GPD1*	Glycerol-3-phosphate dehydrogenase [NAD(+)], cytoplasmic	6.9/37.6	488	8/20	–1.7	369^a	637^b	483^{ab}	194	0.04
120	*PRDX6*	Peroxiredoxin-6	5.7/25.0	390	7/44	–1.2	221^a	262^b	218^a	33	0.03
102	*HSPB1*	Heat shock protein β-1	6.3/22.9	529	12/31	–1.7	360^a	601^b	447^{ab}	173	0.03
108	*HSPB1*	Heat shock protein β-1	6.3/22.9	290	5/28	1.6	159^a	99^b	101^b	38	0.01
440	*TF*	Serotransferrin	7.1/76.9	1,382	28/36	–1.4	444^a	618^b	368^a	162	0.02
31	*MB*	Myoglobin	6.9/17.1	682	32/64	–1.4	4,686^a	6,345^b	5,247^{ab}	1,242	0.04
300	*ACTA2*	Actin, aortic smooth muscle	5.1/42.0	600	13/30	–1.4	174^a	251^b	178^a	48	0.01

^{a,b}Within a row, means without a common superscript differ ($P < 0.05$).

[1]Spot numbering as shown in Fig. 1.

[2]Protein name and accession numbers were derived from the National Center for Biotechnology Information database (http://www.ncbi.nlm.nih.gov; accessed 9 October 2012).

[3]pI = isoelectric point; Mr = molecular weight.

[4]Score from MASCOT (Mascot server version 2.2; http://www.matrixscience.com; accessed 9 October 2012).

[5]MP = the number of matched peptides in the database search; Sc = protein sequence coverage of the matched peptides in relation to the full-length sequence.

[6]Ratio between spot relative volumes of RFI$^-$ and RFI$^+$ pigs. Ratios are inversed and preceded by a minus sign for values lower than 1.

[7]Values are least squares means.

[8]RSD = residual SD (corresponding to the root-mean-square error of the full ANOVA model).

gradient generated across the inner mitochondrial membrane. Other genes encoding proteins implicated in the mitochondrial electron transport chain such as *ND1*, *ND2*, *ND4*, *NDUFB9*, *CYCS*, and *ETFB* were also found to be underexpressed in RFI$^-$ compared with RFI$^+$ animals using the transcriptomic analysis. Finally, proteomic data showed less creatine kinase S-type (CKMT2) in RFI$^-$ pigs. The CKMT2 is a mitochondrial creatine kinase responsible for the transfer of high-energy phosphate to creatine, which plays a central role in energy transport in tissues with large and fluctuating energy demands such as skeletal muscle (Qin et al., 1999). Importantly, this lower oxidative capacity of RFI$^-$ pigs compared with RFI$^+$ pigs postulated here based on transcriptomic and proteomic changes in response to RFI selection is supported by enzymatic data previously obtained in a larger group of pigs from the same generation (Le Naou et al., 2012); lower specific activities of citrate synthase, an indicator of mitochondrial oxidative capacity, and of hydroxy-acyl-CoA dehydrogenase, an indicator of fatty acid β-oxidation potential, have been demonstrated in LM of RFI$^-$ pigs compared with RFI$^+$ pigs (Le Naou et al., 2012). On the other hand, Grubbs et al. (2013b) found a greater abundance of the dihydrolipoyl dehydrogenase, aconitate hydratase, and ATP synthase in isolated mitochondria from the red portion of the semitendinosus muscle of RFI$^-$ pigs compared with RFI$^+$ pigs. Discrepancies between studies are likely due to the fact that Grubbs and colleagues studied intrinsic mitochondrial composition, whereas our results included both differences in mitochondria content as well as differences in their intrinsic composi-

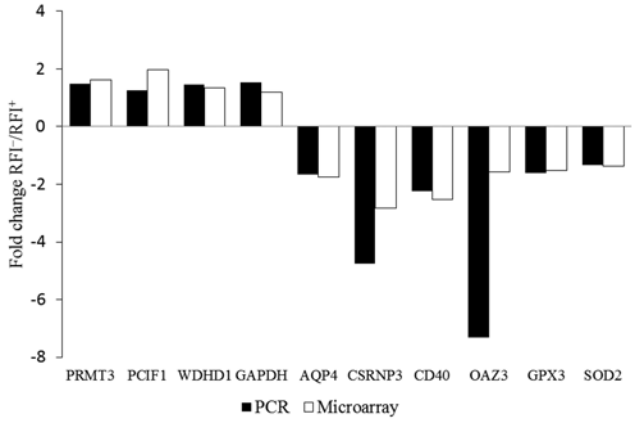

Figure 2. Comparison of microarray and quantitative real-time PCR (qPCR) data for gene expression ratio between low (RFI$^-$) and high (RFI$^+$) residual feed intake pigs in LM. Ratios lower than 1 were expressed as negative numbers (i.e., a ratio of 0.5 is expressed as –2). All significant differences between RFI$^-$ and RFI$^+$ microarray data ($P < 0.01$) were confirmed by qPCR data ($P < 0.05$), except for *superoxide dismutase 2* (*SOD2*; $P = 0.08$). *AQP4 = aquaporin 4*; *CD40 = CD40 molecule TNF receptor superfamily member 5*; *CSRNP3 = cysteine-serine-rich nuclear protein 3*; *GAPDH = glyceraldehyde-3-phosphate dehydrogenase*; *GPX3 = glutathione peroxidase 3*; *OAZ3 = ornithine decarboxylase antizyme 3*; *PCIF1 = phosphorylated CTD-interacting factor 1*; *PRMT3 = protein arginine methyltransferase 3*; *WDHD1 = WD repeat and HMGbox DNA binding protein 1*.

tion. The responses of energy metabolism to selection for RFI might be also different between muscle types.

The current study also indicates that the genetic selection for RFI induces changes in the expression levels of various genes and proteins related to vascularization. The proteomic approach reported lower amount of TF, MB, and ACTA2 in RFI$^-$ pigs than in RFI$^+$ pigs. TF is an iron binding transport protein that is responsible for the transport of iron in the plasma from sites of absorption to sites of storage and utilization, such as in the heme prosthetic group of hemoglobin, myoglobin and cytochromes. MB serves as a transporter of oxygen within muscle fibers and its decrease in RFI$^-$ pigs compared with RFI$^+$ pigs is then consistent with the reduced oxidative metabolism in the LM of RFI$^-$ pigs. Finally, ACTA2 is a vascular smooth muscle actin present in blood vessel walls and its lower abundance in RFI$^-$ pigs could be related with a reduced amount of blood vessels (Fatigati and Murphy, 1984), in accordance with the lower muscle oxidative metabolism in those pigs. The *VEGFA* gene, a member of the PDGF/VEGF growth factor family encoding a protein that acts on endothelial cells and induces angiogenesis and vasculogenesis (Neufeld et al., 1999), was also underexpressed in RFI$^-$ pigs compared with RFI$^+$ pigs by the transcriptomic approach. These differences in muscle oxidative capacity and vascularization may result from selection-induced differences in physical activity, as muscle oxidative metabolism is known to be stimulated by long term physical activity (Pette and Staron, 1997) and the importance of VEGF in regulating skeletal muscle capillarity has been emphasized in studies dealing with adaptation to exercise (Richardson et al., 2000) and stimulated skeletal muscle (Hang et al., 1995). In support, RFI$^-$ pigs have been shown to exhibit a lower physical activity resulting from a lower eating frequency, a shorter daily feeding time (De Haer et al., 1993; Meunier-Salaün et al., 2014), and a lower standing time (Meunier-Salaün et al., 2014).

Besides the downregulation of oxidative metabolism in LM of RFI$^-$ vs. RFI$^+$ pigs, the current transcriptomic and proteomic data also suggest an upregulation of the glycolytic metabolism in RFI$^-$ pigs. Indeed, there was an increase in the expression of GAPDH, a glycolytic enzyme, both at the transcriptional and protein levels in those pigs and a greater abundance of ALDOA evidenced only at the protein level. This higher expression of glycolytic enzymes in muscle of RFI$^-$ pigs is in agreement with the higher percentage of fast-twitch glycolytic fibers previously reported in the same muscle after 4 generations of selection (Lefaucheur et al., 2011). However, previous studies reported a reduced activity of lactate dehydrogenase, an enzyme involved in the terminal route of glycolysis, in LM of pigs selected for RFI$^-$ suggesting reduced glycolysis in those pigs (Le Naou et al., 2012; Faure et al., 2013). Using a proteomic approach, Grubbs et al. (2013b) also found a lower abundance of LDHA in the mitochondrial fraction of LM from RFI$^-$ pigs but the fact that LDHA is a cytosolic protein prompts us to be careful in interpreting those results. Altogether, the effects of RFI selection on muscle glycolytic metabolism remain rather unclear and deserve further study.

Data are Consistent with a Lower Oxidative Stress and Apoptosis in Low-RFI Pigs

The current study highlights the downregulation of 3 molecules involved in cell defense against ROS in RFI$^-$ pigs compared with RFI$^+$ pigs. Peroxiredoxin-6 was decreased at the protein level, whereas SOD2 and GPX3 exhibited decreased mRNA levels. Because the metabolic challenge during physical exercise results in an elevated generation of ROS (Bo et al., 2013), the observed greater levels of antioxidant molecules in the muscle of RFI$^+$ pigs could be an adaptive mechanism to cope with a higher and deleterious ROS production (Radak et al., 2005). In accordance, a greater ROS production has been reported in mitochondria from semitendinosus muscle in RFI$^+$ pigs (Grubbs et al., 2013a) and from breast muscle in broilers with low feed efficiency (Bottje and Carstens, 2009). Furthermore, the mitochondria protein profile in LM indicated a greater abundance of proteins in-

volved in oxidative and antioxidative stress in the less efficient RFI^+ line (Grubbs et al., 2013b). Therefore, available data suggest that muscle of RFI^- pigs may have less mitochondria, which would be intrinsically more efficient and less prone to produce ROS than those of RFI^+ pigs. In the present experiment, GPD1 showed a higher abundance in RFI^+ than RFI^- pigs at the protein level. This enzyme could counterbalance ROS production in RFI^+ pigs while maintaining a high oxidative metabolism. Indeed, GPD1 plays a critical role in carbohydrate and lipid metabolism by catalyzing the reversible conversion of dihydroxyacetone phosphate and NADH to glycerol-3-phosphate and NAD+ in the cytoplasm. Importantly, GPD1 is part of the glycerol phosphate shuttle that facilitates the transfer of reducing equivalents generated during glycolysis in the cytosol (NADH) to coenzyme Q in the mitochondrial electron transport chain, transferring cytoplasmic reducing equivalents through flavin adenine dinucleotide (**$FADH_2$**) directly to complex II, thus bypassing complex I, a site where ROS are generated. The global reaction is exothermic, driven by the difference in free energy between NADH in the cytosol and reduced $FADH_2$ in the mitochondria, which could contribute to the greater feed efficiency and lower heat loss of RFI^- pigs than of RFI^+ pigs (Barea et al., 2010). The underexpression of *OAZ3*, an inhibitor of ornithine decarboxylase, in RFI^- vs. RFI^+ pigs could also improve the antioxidative defense in RFI^- pigs because ornithine decarboxylation is the first step in the synthesis of polyamines that are important as antioxidants. Moreover, *cysteine-serine-rich nuclear protein 3* (*CSRNP3*), a transcriptional factor involved in apoptosis, was also underexpressed at the mRNA level in RFI^- pigs. Altogether, available data suggest a reduced ROS production in LM of the RFI^- pigs, which might be also associated with lower oxidative stress and apoptosis compared with RFI^+ pigs.

Transcriptomic Data Suggest a Greater Muscle Protein Synthesis in Low-RFI Pigs

Transcriptomic data highlighted differences in the expression of some genes involved in protein synthesis or degradation. Notably, genes encoding initiation and elongation translation factor subunits (*EEF1A1*, *EEF1G*, *EIF2S2*, *EIF2B5*, and *EIF6*), and *type I protein arginine N-methyltransferase* (*PRMT3*) involved in the maturation of the 80 and 56S ribosomal proteins were overexpressed in RFI^- vs. RFI^+ pigs. Feed restriction may also affect some genes in protein metabolism. Indeed, protein synthesis and protein catabolic pathways were simultaneously enriched in RFI^{+R} pigs when compared with RFI^+ pigs. However, it remains elusive to relate these changes observed at the mRNA levels to differences in carcass lean meat content reported between the different groups. Indeed, we failed to identify any differences between lines or due to feed restriction for the relative abundance in these proteins using the proteomic approach. Similarly, it has been reported that markers of protein synthesis did not differ between 2 Yorkshire pig lines selected for divergent feed efficiency (Cruzen et al., 2013). Except for the gene encoding for the millimolar-calpain protease (CAPN2) involved in muscle protein degradation, which was overexpressed in RFI^- animals compared with RFI^+ animals, expression levels of other genes linked to protein catabolism were not modified by selection in the current study. These latter observations are consistent with the lack of difference in activities of enzymes involved in protein catabolism (calpains and proteasome) reported recently on a larger group of animals from the same experiment (Le Naou et al., 2012). On the other hand, an increased activity of the calpastatin, an endogenous calpain (calcium-dependent cysteine protease) inhibitor, and a decreased 20S proteasome protein degradation systems have been reported in muscle of a RFI^- versus a RFI^+ pig line (Cruzen et al., 2013), suggesting a lower protein degradation rate in RFI^- pigs. A reduction in the rate of protein breakdown along with a higher level of calpastatin has been reported in a RFI^- line of cattle (McDonagh et al., 2001). We have no particular explanation for the discrepancies between our study and other studies, except the fact that different techniques were used. Le Naou et al. (2012) measured overall 26S proteasome activity (association of 20S subunit with 1 or 2 19S regulatory complexes), whereas Cruzen et al. (2013) measured the proteolytic core complex 20S. Altogether, further studies are needed to clarify the effects of RFI selection on protein turnover.

Finally, translation needs abundant sources of energy, particularly ATP, which is essentially produced by oxidative metabolism and phosphorylation in mitochondria. When reducing equivalents produced by fatty acid oxidation and tricarboxylic acid cycle are oxidized, both ATP and ROS are produced, and ROS production may limit ATP production. In the present study, superoxide dismutase and glutathione peroxidase 3 at the mRNA level and peroxiredoxin 6 at the protein level were found to be underexpressed in RFI^- pigs, which could reflect a lower ROS production in these pigs. In support, recent studies by Bottje and Carstens (2009) and Grubbs et al. (2013a) also showed that genetic selection for RFI^- attenuates H_2O_2 production in mitochondria, limiting ROS production.

Conclusion

Divergent selection for RFI during 7 generations modified gene and protein expressions in pig muscle, so that RFI$^-$ pigs exhibited a lower oxidative metabolism in muscle. This was associated with the downregulation of antioxidative molecules, which could reflect a lower muscular oxidative stress in those pigs. The greater lean meat proportion induced by selection in RFI$^-$ pigs might be related to a more efficient energy metabolism in muscle, enabling a shift in energy utilization toward lean growth as suggested by the overexpression of genes involved in protein synthesis. The comparisons made in the present study by considering an additional feed-restricted RFI$^+$ group indicated that differences between RFI lines were likely not related to differences in feed intake per se. A recent study suggests that the adenosine monophosphate–activated protein kinase pathway could be involved in the underlying mechanisms linking the numerous changes induced by divergent selection on RFI in skeletal muscle (Faure et al., 2013) but further studies are needed to establish these relationships.

LITERATURE CITED

Barea, R., S. Dubois, H. Gilbert, P. Sellier, J. van Milgen, and J. Noblet. 2010. Energy utilization in pigs selected for high and low residual feed intake. J. Anim. Sci. 88:2062–2072. doi:10.2527/jas.2009-2395

Bo, H., N. Jiang, L. L. Ji, and Y. Zhang. 2013. Mitochondrial redox metabolism in aging: Effect of exercise interventions. J. Sport Health Sci. 2:67–74. doi:10.1016/j.jshs.2013.03.006

Bottje, W. G., and G. E. Carstens. 2009. Association of mitochondrial function and feed efficiency in poultry and livestock species. J. Anim. Sci. 87(E. Suppl.):E48–E63.

Casel, P., F. Moreews, S. Lagarrigue, and C. Klopp. 2009. SigReannot: An oligo-set re-annotation pipeline based on similarities with the Ensembl transcripts and Unigene clusters. BMC Proc. 3(Suppl. 4):S3.

Colinet, H., D. Renault, B. Charoy-Guevel, and E. Com. 2012. Metabolic and proteomic profiling of diapause in the aphid parasitoid praon volucre. PLoS ONE 7:e32606. doi:10.1371/journal.pone.0032606

Cruzen, S. M., A. J. Harris, K. Hollinger, R. M. Punt, J. K. Grubbs, J. T. Selsby, J. C. M. Dekkers, N. K. Gabler, S. M. Lonergan, and E. Huff-Lonergan. 2013. Evidence of decreased muscle protein turnover in gilts selected for low residual feed intake. J. Anim. Sci. 91:4007–4016. doi:10.2527/jas.2013-6413

De Haer, L. C. M., P. Luiting, and H. L. M. Aarts. 1993. Relations among individual (residual) feed intake, growth-performance and feed-intake pattern of growing pigs in-group housing. Livest. Prod. Sci. 36:233–253. doi:10.1016/0301-6226(93)90056-N

Dennis, G., B. T. Sherman, D. A. Hosack, J. Yang, W. Gao, H. C. Lane, and R. A. Lempicki. 2003. DAVID: Database for annotation, visualization, and integrated discovery. Genome Biol. 4:R60. doi:10.1186/gb-2003-4-9-r60

Fatigati, V., and R. A. Murphy. 1984. Actin and tropomyosin variants in smooth muscles – Dependence on tissue type. J. Biol. Chem. 259:4383–4388.

Faure, J., L. Lefaucheur, N. Bonhomme, P. Ecolan, K. Meteau, S. M. Coustard, M. Kouba, H. Gilbert, and B. Lebret. 2013. Consequences of divergent selection for residual feed intake in pigs on muscle energy metabolism and meat quality. Meat Sci. 93:37–45. doi:10.1016/j.meatsci.2012.07.006

Gilbert, H., J. P. Bidanel, J. Gruand, J. C. Caritez, Y. Billon, P. Guillouet, H. Lagant, J. Noblet, and P. Sellier. 2007. Genetic parameters for residual feed intake in growing pigs, with emphasis on genetic relationships with carcass and meat quality traits. J. Anim. Sci. 85:3182–3188. doi:10.2527/jas.2006-590

Grubbs, J. K., A. N. Fritchen, E. Huff-Lonergan, J. C. M. Dekkers, N. K. Gabler, and S. M. Lonergan. 2013a. Divergent genetic selection for residual feed intake impacts mitochondria reactive oxygen species production in pigs. J. Anim. Sci. 91:2133–2140. doi:10.2527/jas.2012-5894

Grubbs, J. K., A. N. Fritchen, E. Huff-Lonergan, N. K. Gabler, and S. M. Lonergan. 2013b. Selection for residual feed intake alters the mitochondria protein profile in pigs. J. Proteomics 80:334–345. doi:10.1016/j.jprot.2013.01.017

Hang, J., L. Kong, J. W. Gu, and T. H. Adair. 1995. VEGF gene expression is upregulated in electrically stimulated rat skeletal muscle. Am. J. Physiol. 269:H1827–H1831.

Huang, D. W., B. T. Sherman, R. Stephens, M. W. Baseler, H. C. Lane, and R. A. Lempicki. 2008. DAVID gene ID conversion tool. Bioinformation 2:428–430. doi:10.6026/97320630002428

Hwang, I. H., B. Y. Park, J. H. Kim, S. H. Cho, and J. M. Lee. 2005. Assessment of postmortem proteolysis by gel-based proteome analysis and its relationship to meat quality traits in pig longissimus. Meat Sci. 69:79–91. doi:10.1016/j.meatsci.2004.06.019

Le Naou, T., N. Le Floc'h, I. Louveau, H. Gilbert, and F. Gondret. 2012. Metabolic changes and tissue responses to selection on residual feed intake in growing pigs. J. Anim. Sci. 90:4771–4780. doi:10.2527/jas.2012-5226

Lefaucheur, L., B. Lebret, P. Ecolan, I. Louveau, M. Damon, A. Prunier, Y. Billon, P. Sellier, and H. Gilbert. 2011. Muscle characteristics and meat quality traits are affected by divergent selection on residual feed intake in pigs. J. Anim. Sci. 89:996–1010. doi:10.2527/jas.2010-3493

Lkhagvadorj, S., L. Qu, W. Cai, O. P. Couture, C. R. Barb, G. J. Hausman, D. Nettleton, L. L. Anderson, J. C. M. Dekkers, and C. K. Tuggle. 2010. Gene expression profiling of the short-term adaptive response to acute caloric restriction in liver and adipose tissues of pigs differing in feed efficiency. Am. J. Physiol. Regul. Integr. Comp. Physiol. 298:R494–R507. doi:10.1152/ajpregu.00632.2009

McDonagh, M. B., R. M. Herd, E. C. Richardson, V. H. Oddy, J. A. Archer, and P. F. Arthur. 2001. Meat quality and the calpain system of feedlot steers following a single generation of divergent selection for residual feed intake. Aust. J. Exp. Agric. 41:1013–1021. doi:10.1071/EA00024

Meunier-Salaün, M. C., C. Guérin, Y. Billon, P. Sellier, J. Noblet, and H. Gilbert. 2014. Divergent selection for residual feed intake in group-housed growing pigs: Characteristics of physical and behavioural activity according to line and sex. Animal 8:1898–1906. doi:10.1017/S1751731114001839

Neufeld, G., T. Cohen, S. Gengrinovitch, and Z. Poltorak. 1999. Vascular endothelial growth factor (VEGF) and its receptors. FASEB J. 13:9–22.

Pette, D., and R. S. Staron. 1997. Mammalian skeletal muscle fiber type transitions. Int. Rev. Cytol. 170:143–223. doi:10.1016/S0074-7696(08)61622-8

Pfaffl, M. W. 2001. A new mathematical model for relative quantification in real-time RT-PCR. Nucleic Acids Res. 29:e45. doi:10.1093/nar/29.9.e45

Qin, W. N., Z. Khuchua, J. Boero, R. M. Payne, and A. W. Strauss. 1999. Oxidative myocytes of heart and skeletal muscle express abundant sarcomeric mitochondrial creatine kinase. Histochem. J. 31:357–365. doi:10.1023/A:1003748108062

R Development Core Team. 2008. R: A language and environment for statistical computing. R Foundation for Statistical Computing, Vienna, Austria. http://www.R-project.org. (Accessed 8 December 2011.)

Radak, Z., H. Y. Chung, and S. Goto. 2005. Exercise and hormesis: Oxidative stress-related adaptation for successful aging. Biogerontology 6:71–75. doi:10.1007/s10522-004-7386-7

Richardson, E. C., and R. M. Herd. 2004. Biological basis for variation in residual feed intake in beef cattle. 2. Synthesis of results following divergent selection. Aust. J. Exp. Agric. 44:431–440. doi:10.1071/EA02221

Richardson, R. S., H. Wagner, S. R. D. Mudaliar, E. Saucedo, R. Henry, and P. D. Wagner. 2000. Exercise adaptation attenuates VEGF gene expression in human skeletal muscle. Am. J. Physiol. Heart Circ. Physiol. 279:H772–H778.

Schlicker, A., F. S. Domingues, J. Rahnenführer, and T. Lengauer. 2006. A new measure for functional similarity of gene products based on Gene Ontology. BMC Bioinformatics 7:302.

Supek, F., M. Bosnjak, N. Skunca, and T. Smuc. 2011. REVIGO Summarizes and visualizes long lists of gene ontology terms. PLoS ONE 6:e21800. doi:10.1371/journal.pone.0021800

Vandesompele, J, K. De Preter, F. Pattyn, B. Poppe, N. Van Roy, A. De Paepe, and F. Speleman. 2002. Accurate normalization of real-time quantitative RT-PCR data by geometric averaging of multiple internal control genes. Genome Biol. 3:RESEARCH0034.

Vincent, A., I. Louveau, F. Gondret, B. Lebret, and M. Damon. 2012. Mitochondrial function, fatty acid metabolism, and immune system are relevant features of pig adipose tissue development. Physiol. Genomics 44:1116–1124. doi:10.1152/physiolgenomics.00098.2012